Chem. Res. Chin. Univ., 2017, 33(4), 530—533 doi: 10.1007/s40242-017-6261-4

Preparation of Fe_3O_4-porphyrin Nano-composited Particles and Their Optical and Magnetic Properties

GUO Ximing[1*] and GUO Bin[2]

1. School of Life Science of Technology Institution, Harbin Institute of Technology, Harbin 150001, P. R. China;
2. School of Materials Science and Engineering Institution, Harbin Institute of Technology, Harbin 150001, P. R. China

Abstract Magnetic Fe_3O_4 nanoparticles were synthesized *via* the coprecipitation of ferrous and ferric ion. The morphology and magnetic properties of the magnetic Fe_3O_4 nanoparticles were investigated by transmission electron microscopy(TEM) and superconducting quantum interference device. Furthermore, the Fe_3O_4-porphyrin nanocomposite particles(FeOPNCPs) are prepared with Fe_3O_4 and porphyrin by sol-gel method. The patterns of FeOPNCPs were also characterized by means of scanning electron microscopy(SEM) and TEM. The optical and magnetic properties of FeOPNCPs were investigated on a UV-Vis spectrophotometer, a fluorescence spectrophotometer and a superconducting quantum interference device. These experimental results show that FeOPNCPs not only possess optical features of porphyrin but also retain the superparamagnetic features of Fe_3O_4 nanoparticles.

Keywords Fe_3O_4; Porphyrin; Nano-composited particle; Fluorescence; Magnetic property

1 Introduction

Magnetic optical bifunctional nanoparticles[1,2] have been used for fluorescence labelling and magnetic separation in biomedical fields[3—5]. Magnetic optical bifunctional nanoparticles can be not only easily manipulated by the exterior magnetic field but also synchronously observed by the fluorescence imaging technology. Therefore, magnetic optical bifunctional nanoparticles have more extensively application than the single-functional nanoparticles in many fields including bio-pharmaceutical[6], bioassay, drug delivery[7], biomarkers[8], biosensors, and so on. Up to now, various different magnetic optical bifunctional nanoparticles have been reported[9—11]. However, the magnetic optical bifunctional nanoparticles have been applied in the biomedical fields, which require magnetic optical bifunctional nanoparticles with high brightness and strong magnetic as well as a proper size, low toxicity and good dispersion in aqueous phase. The magnetic optical bifunctional nanoparticles have been strictly limited in biomedicine because there are still a lot of problems to be solved[12]. So it is worth exploring suitable magnetic optical bifunctional nanoparticles to meet the requirements of bio-application. Porphyrin is a class of synthetic and natural 18π electron structural macrocyclic compounds and porphyrin periphery is easily decorated by different substituents. Porphyrin has been developed as the photosensitive drugs in photodynamic diagnose and therapy in clinically superficial malignant tumor treatment. Although many advanced functional materials with well-defined shapes and dimensions have been built up based on porphyrin itself, many other multifunctional materials can also be constructed from porphyrin, as basic building blocks, combined with other functional materials. Magnetic fluid is a kind of highly stable colloidal solution and the ferromagnetic or ferrimagnetism nanoparticles can be dispersed in it. Magnetic Fe_3O_4 fluids have shown good bio-application prospects in many fields. When the diameters of magnetic Fe_3O_4 nanoparticles are less than 20 nm, the Fe_3O_4 magnetic fluid displays good superparamagnetic features and have been widely applied in biological detection[13], sensor[14], drug delivery[15], immobilized enzyme[16], and so on. In this report, magnetic optical bifunctional nanocomposite particles were synthesized based on Fe_3O_4 and porphyrin *via* sol-gel method. The patterns of Fe_3O_4-porphyrin nanocomposite particles(FeOPNCPs) were characterized by means of scanning electron microscopy(SEM) and transmission electron microscopy(TEM). The optical and magnetic properties of FeOPNCPs were investigated by UV-Vis, fluorescence spectroscopy and superconducting quantum interference device.

2 Experimental

2.1 Reagents and Instruments

The synthesis procedures of tetrakis-p-hydroxylphenylporphyrin(THPP), Fe_3O_4, acetyl chloride and siloxane bonding porphyrin were reported in refs.[17—19]. Other chemical reagents were bought from Shanghai and Tianjin chemical

*Corresponding author. E-mail: ximingguo@hit.edu.cn

Received June 22, 2016; accepted November 8, 2016.

Supported by the Fundamental Research Funds from the Central Universities of China, the Natural Scientific Research Innovation Foundation of Harbin Institute of Technology, China(Nos.HIT.IBRSEM.2009.003, HIT.ICRST.2010012), the Ministry of Science and Technology International Cooperation Project, China(No.2012DFR30220) and the National Natural Science Foundation of China(No.514070467).

reagent companies. Fourier Transform infrared spectra(FTIR) were measured on a 1730 FTIR infrared spectrometer; UV-Vis spectra were measured on a Hitachiu-3900 ultraviolet-visible spectrophotometer; SEM measurement was performed on a Quanta 200F instrument, TEM measurement was carried out on a Hitachi-7650 instrument; magnetic data were collected on a superconducting quantum interference device(MPMS-X-7). X-Ray photoelectron spectra(XPS) were measured on a Rigaku D/Max 2500 v/PC instrument. Laser scanning confocal microscopy was performed on a Zeiss 510 Laser scanning confocal microscope(LSCM) with 480 nm as the excitation wavelength.

2.2 Preparation of FeOPNCPs

The preparation routes of FeOPNCPs are displayed in Scheme 1. 0.44 g of (2-ethylhexyl) succinate sodium sulfate (AOT) and 600 μL of *n*-butyl alcohol were dissolved in 20 mL of deionized water under the mechanical stirring and 10 mL of 7.5 mg/mL magnetic Fe_3O_4 dispersed solutions was added to the reaction system after the ultrasonic treatment for 15 min. Then 15 mL of *N,N*-dimethylformamide(DMF) including 50 mg of siloxane bonding porphyrin was slowly added to the system. The reaction solutions were continuously treated for

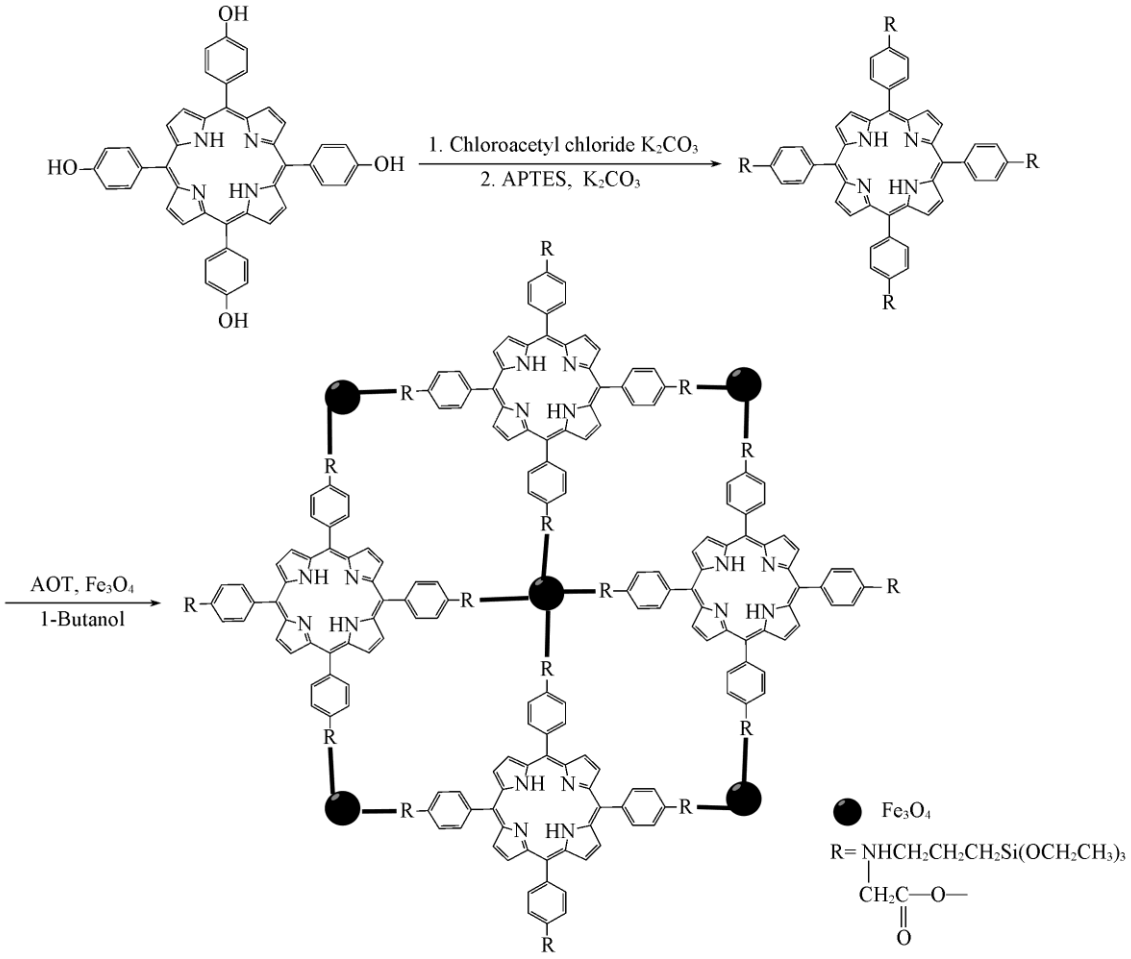

Scheme 1 Preparation routes of FeOPNCPs

1 h in an ultrasonic bath. FeOPNCPs powders were collected and held with DMF and deionized water under a constant external magnetic field. Then FeOPNCPs were ultrasonically dispersed into 20 mL of DMF.

3 Results and Discussion

3.1 Surface Properties of Magnetic Fe_3O_4 Nanoparticles

Surface properties of magnetic Fe_3O_4 nanoparticles are investigated by XPS and the results are displayed in Fig.1. The peaks of $Fe_{2p3/2}$ and $Fe_{2p1/2}$ in Fe_3O_4 nanoparticles are located at 711.1 and 724.7 eV, respectively, showing that the nonequivalent Fe components exist in different chemical environments in Fe_3O_4 nanoparticles. $Fe_{2p3/2}$ peak at 711.1eV can be legitimately fitted to two peaks at 710.38 and 711.99 eV, which are assigned to the typical peak of FeOOH and face-centered cubic Fe_3O_4

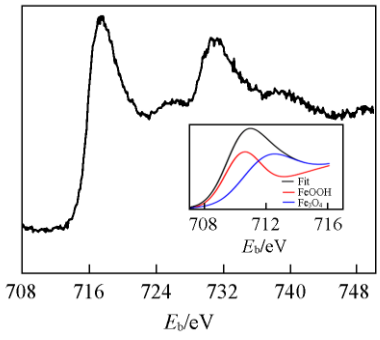

Fig.1 XPS spectra of the magnetic Fe_3O_4 nanoparticles
Inset: the peaks in different chemical environments.

structure according to NIST XPS Database(Version 4.1) and the literature[20,21].

3.2 UV-Vis Analysis of Porphyrin and FeOPNCPs

Fig.2 shows UV-Vis spectra of porphyrin and FeOPNCPs in DMF. A strong Soret absorption band appears at 419 nm and four weak Q absorption bands appear at 515, 552, 592 and 649 nm in the UV-Vis spectrum of porphyrin, respectively[21]. However, the UV-Vis spectrum of FeOPNCPs only shows the Soret absorption band of porphyrin, the four Q absorption bands of porphyrin are very weak. The UV-Vis spectrum of FeOPNCPs slopes due to the strong scattering effect of Fe_3O_4 nanoparticles in UV-Vis range, which indirectly illustrates that porphyrin has been attached on the surface of Fe_3O_4 nanoparticles and FeOPNCPs have been formed. The strong scattering effect of Fe_3O_4 nanoparticles resulted from the typical Q absorption band of porphyrin can be concealed in the UV-Vis spectrum of FeOPNCPs.

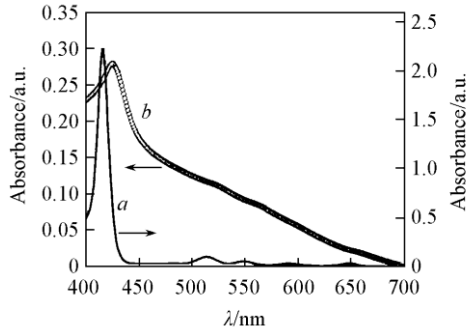

Fig.2 UV-Vis spectra of porphyrin in DMF(*a*) and FeOPNCPs in water(*b*)

3.3 FTIR Spectra of Fe_3O_4 and FeOPNCPs

Fig.3 shows the FTIR spectra of magnetic Fe_3O_4 and FeOPNCPs. In the FTIR spectra of magnetic Fe_3O_4, the vibration peak appearing at 3454 cm^{-1} can be assigned to the stretching vibration of FeOOH and the adsorbed water on the surface of Fe_3O_4; the vibration peak at 1652 cm^{-1} can be assigned to the adsorbed water on the surface of Fe_3O_4; the vibration peak at 594 cm^{-1} can be assigned to the Fe—O characteristic vibration of Fe_3O_4[22]. However, in the FTIR spectra of FeOPNCPs, a broad vibration peak at 3456 cm^{-1} and a shoulder peak at 3330 cm^{-1} can be assigned to the N—H stretching vibration of amide bond and the N—H stretching vibration of porphyrin. The peaks at 2952 and 2873 cm^{-1} are assigned to the corresponding C—H stretching vibration of methylene and benzene ring of porphyrin. The peaks at 1612, 1468, 998, 720 and 540 cm^{-1} are attributed to the porphyrin skeleton vibration. The vibration peak at 1080 cm^{-1} is owing to the typical Si—O characteristic vibration. FTIR data further confirm the structure of FeOPNCPs.

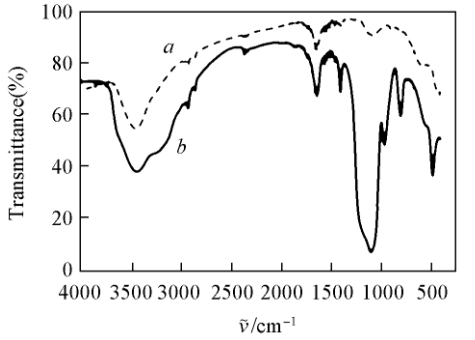

Fig.3 FTIR spectra of Fe_3O_4(*a*) and FeOPNCPs(*b*)

3.4 SEM and TEM Measurements of FeOPNCPs

The morphologies of FeOPNCPs observed by SEM and TEM are shown in Fig.4. The morphology of FeOPNCPs is approximately spherical and a network crosslinking structure has been formed[Fig.4(A)]. In order to clearly observe the network crosslinking structure of FeOPNCPs, the TEM image of FeOPNCPs is displayed in Fig.4(B) and the amplification image is inserted in it. FeOPNCPs show a typical amorphous nebular structure. Magnetic Fe_3O_4 nanoparticles have anchored into the amorphous nebular structure and fixed tightly, which would effectively avoid the accumulation of magnetic Fe_3O_4 nanoparticles after the formation of FeOPNCPs(Fig.4).

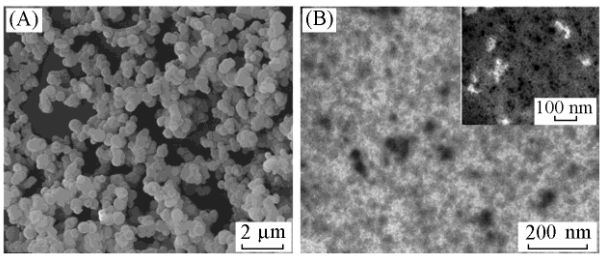

Fig.4 SEM(A) and TEM(B) images of FeOPNCPs
Inset of (B): amplification image.

3.5 Magnetic Properties of Fe_3O_4 and FeOPNCPs

At 310 K, the hysteresis loops of Fe_3O_4 and FeOPNCPs were carried out on a superconducting quantum interference device, which are displayed in Fig.5. The saturated magnetic intensity of the magnetic Fe_3O_4 nanoparticles is about 27.4 $A \cdot m^2/kg$ and the saturated magnetic intensity of FeOPNCPs is about 10.8 $A \cdot m^2/kg$. The saturated magnetic intensity of FeOPNCPs is lower than that of the Fe_3O_4 nanoparticles, which could be attributed to the following two cases. On the one hand, the decreases of the absolute content of magnetic Fe_3O_4 nanoparticles result in the decreases of the saturated magnetic intensity of FeOPNCPs. On the other hand, Si—O groups have been modified on the Fe_3O_4 nanoparticles surface, and the particle size and specific surface properties of the magnetic

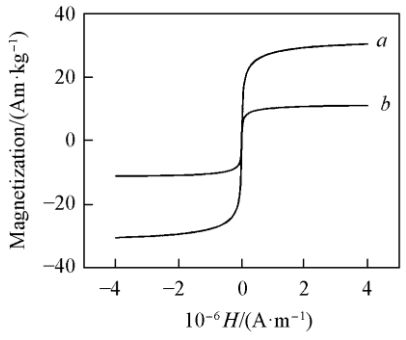

Fig.5 Magnetic properties of Fe_3O_4(*a*) and FeOPNCPs(*b*)

Fe_3O_4 nanoparticles are changed, which could cause the decrease of the saturated magnetic intensity of FeOPNCPs. These results further imply that FeOPNCPs have been successfully prepared. Furthermore, the hysteresis loop of FeOPNCPs is identical with that of the magnetic Fe_3O_4 particles, which displays that FeOPNCPs maintain good superparamagnetic features of the magnetic Fe_3O_4 nanoparticles.

3.6 Fluorescence Spectra of Porphyrin and FeOPNCPs

Fig.6 shows the fluorescence spectra of porphyrin in DMF and FeOPNCPs in water. The maximum emission peak of porphyrin appears at 650 nm and the maximum emission peak of FeOPNCPs appears at 660 nm when the excited wavelength being 410 nm. The maximum emission peak of FeOPNCPs red-shifts about 10 nm relative to that of porphyrin and the intensity is far lower than that of porphyrin, which can be reasonably explained as follows. The strong electronic interactions between FeOOH on the surface of magnetic Fe_3O_4 nanoparticles and porphyrin have strong quenching effect on the fluorescence of porphyrin when forming FeOPNCPs. In addition, the fluorescence peak at approximate 720 nm cannot be observed in porphyrin, but a relatively strong fluorescence peak at 724 nm can be observed in FeOPNCPs, which can be attributed to two possible reasons. First, the emission peak intensity at 650 nm is greatly stronger than that at *ca.*720 nm, which leads to the result that the fluorescence peak at *ca.* 720 nm is concealed in the fluorescence spectra of porphyrin. The fluorescence intensity at 650 nm is strictly quenched by Fe_3O_4 and the fluorescence intensity at 720 nm has not been influenced when forming FeOPNCPs. Second, the energy levels of porphyrin are splitted due to the micro-environmental change of it when it is modified on the surface of Fe_3O_4 nanoparticles, which can result in the strong fluorescence peak at 724 nm in the fluorescence spectra of FeOPNCPs.

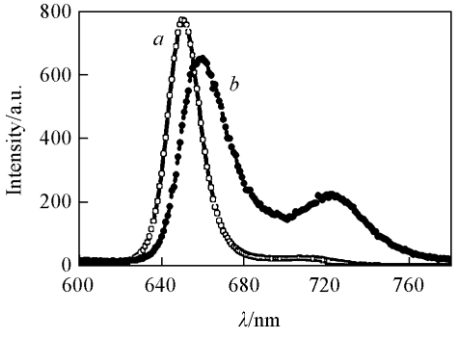

Fig.6 Fluorescence spectra of porphyrin in DMF(*a*) and FeOPNCPs in water(*b*)

3.7 LSCM of FeOPNCPs

In order to further investigate the fluorescence imaging properties of FeOPNCPs, LSCM measurement of FeOPNCPs was performed under the dried condition and the result is displayed in Fig.S1(see the electronic Supplementary Material of this paper). The LSCM image of FeOPNCPs exhibits bright and clear red fluorescence and serious accumulation in dried state.

4 Conclusions

FeOPNCPs have been successfully synthesized from magnetic Fe_3O_4 nanoparticles and porphyrin *via* sol-gel method. The structure and morphology of FeOPNCPs were characterized by means of FTIR, SEM and TEM and the results showed that FeOPNCPs possessed a network structure. The optical and magnetic features of FeOPNCPs were investigated on a UV-Vis spectrophotometer, a fluorescence spectrophotometer and a superconducting quantum interference device, and the results showed that FeOPNCPs retained not only optical properties of porphyrin but also superparamagnetic properties of Fe_3O_4 nanoparticles.

Electronic Supplementary Material

Supplementary material is available in the online version of this article at http://dx.doi.org/10.1007/s40242-017-6261-4.

References

[1] Haynes C. L., van Duyne R. P., *J. Phys. Chem. B*, **2001**, *105*, 5599
[2] Xue Y. C., Zun D. L., *J. Phys.: Condens. Mat.*, **1997**, *9*, 798
[3] Kim H., Achermann M., Balet L. P., Hollingsworth J. A., Klimov V. I., *J. Am. Chem. Soc.*, **2005**, *127*, 544
[4] Yu X., Shan Y., Li G., Chen K., *J. Mater. Chem.,* **2011**, *21*, 8104
[5] Tian Q., Hu J., Zhu Y., Zou R., Chen Z., Yang S., Li R., Su Q., Han Y., Liu X., *J. Am. Chem. Soc.*, **2013**, *135*, 8571
[6] Sun C., Lee J. S., Zhang M., *Adv. Drug Deliv. Rev.*, **2008**, *60*, 1252
[7] Kim J., Kim H. S., Lee N., Kim T., Kim H., Yu T., Song I. C., Moon W. K., Hyeon T., *Angew. Chem. Int. Ed.*, **2008**, *47*, 8438
[8] Gao J., Zhang W., Huang P., Zhang B., Zhang X., Xu B., *J. Am. Chem. Soc.*, **2008**, *130*, 3710
[9] Ma Q., Yu W., Dong X., Wang J., Liu G., Xu J., *Opt. Mater.*, **2013**, *35*, 526
[10] Jiang J., Gu H., Shao H., Devlin E., Papaefthymiou G. C., Ying J. Y., *Adv. Mater.*, **2008**, *20*, 4403
[11] Weller D., Brändle H., Gorman G., Lin C. J., Notarys H., *Appl. Phys. Lett.*, **1992,** *61*, 2726
[12] Pankhurst Q. A., Connolly J., Jones S. K., Dobson J. J., *J. Phys. D: Appl. Phys.*, **2003**, *36*, R167
[13] Liang R. P., Yao G. H., Fan L. X., Qiu J. D., *Anal. Chim. Acta*, **2012**, *737*, 22
[14] Liu Q., Hu L., Zhao Q., Zhu R., Yang Y., Jia Q., Bing B., Zhuo L., *Meas. Sci. Technol.*, **2014**, *41*, 142
[15] Gu L., He X., Wu Z., *Mater. Chem. Phys.*, **2014**, *148*, 153
[16] Li Y. C., Lin Y. S., Tsai P. J., Chen C. T., Chen W. Y., Chen Y. C., *Anal. Chem.*, **2007**, *79*, 7519
[17] Guo X. M., Su L. J., Yu L.X., Shi T. S., *Chem. J. Chinese Universities*, **2006**, *27*(3), 410
[18] Guo X. M., Guo B., Sun X., Zhang Q., Shi T. S., *Chinese J. Chem.*, **2011**, *29*, 363
[19] Guo X. M., Guo B., Zhang Q., Sun X., *Dalton*, **2011**, *40*, 3039
[20] Stohr J., Nakajima R., *J. Res. Dev.*, **1998**, *42*, 73
[21] Guo X. M., Guo B., *J. Phys. Chem.*, **2015**, *19*, 8591
[22] Sudakar C., Subbanna N. G., Kutty N. T., *Journal of Materials Chemistry*, **2002**, *1*, 107